TASK I
Project I.8

ACTIVITY AND SELECTIVITY OF SLURRY PHASE IRON-BASED CATALYSTS FOR MODEL SYSTEMS

Christine W. Curtis
Department of Chemical Engineering
Auburn University

SUMMARY

The activity and selectivity of iron-based slurry-phase catalysts were investigated for the hydrogenation of pyrene and the hydrocracking of C-C bonds in several model compounds: 1-methylnaphthalene (1-MN), 2-hexylnaphthalene (2-HN), and 4-(1-naphthylmethyl)bibenzyl (NMBB). Reactions were performed under typical coal liquefaction conditions. Higher reaction temperature and the presence of sulfur increased the hydrogenation of pyrene by the iron catalysts generated in situ. An in situ method of catalyst addition was most effective for pyrene hydrogenation for the iron catalysts, while molybdemum naphthenate showed increased activity with two-stage processing. Both Fe and Mo catalysts showed low activity in reactions where the catalyst was generated ex situ. Combinations of Fe and Mo catalysts were synergistic for pyrene hydrogenation, although the amount of increase was dependent upon the particular iron precursor used. The Fe and Mo catalysts affected the hydrocracking of the three model species differently. Molybdenum naphthenate was more active for hydrocracking 2-HN and NMBB than any of the Fe catalysts but combining FeNaph with MoNaph was detrimental to the hydrocracking of these compounds. The selectivity of hydrocracking NMBB at specific bonding sites was affected by the presence and type of catalyst, presence of sulfur, and reaction time.

INTRODUCTION

Slurry-phase catalyst precursors that form finely divided catalysts during reactions have been shown to be active for coal liquefaction and coprocessing.[1-4] Addition of Fe catalysts in the form of finely divided Fe (III) oxides and Fe oxyhydroxides modified with either (SO_4^{2-}) or molybdate (MoO_4^{2-}) anions in coal liquefaction increased coal conversion and selectivities to n-pentane soluble products.[4] A bimetallic catalyst that incorporated Mo with Fe, forming $Mo/Fe_2O_3/SO_4^{2-}$ which consisted of 50 ppm Mo and 3500 ppm Fe, was active for coal conversion with a selectivity for oil.[4] Other researchers[5-8] have evaluated the catalytic activities of Fe present in different chemical forms in model coal reactions. Iron catalysts composed of $Fe(CO)_5$ or $Fe(CO)_5$-S had high activity for hydrogenation (HYD) of aromatic species.[4] Iron catalysts composed of Fe (III) oxides, sulfated Fe oxides, or FeOOH have also been shown to be active for hydrocracking (HYC) model compounds such as 4-(1-naphthylmethyl)bibenzyl (NMBB).[6-8] Reactions of NMBB were performed in the presence of a H_2 donor solvent, 9,10-dihydrophenanthrene. Selective bond cleavage occurred, depending on the composition of the Fe catalyst and the presence of water in the system.[8] A series of Fe catalysts generated by different means such as from oil-soluble iron pentacarbonyl, ultrafine ferric oxide and ferric oxyhydroxide, chemical impregnation of Fe catalysts into coal and cation exchange of iron species with coal have been analyzed using ^{57}Fe Mössbauer and X-ray absorption fine structure (XAFS) spectroscopy.[9] The chemical structure of the different catalysts and particle sizes were determined.

The objective of this study was to determine the activity and selectivity of different Fe and Mo catalyst precursors for hydrogenating and hydrocracking model systems such as pyrene (PYR), 1-methylnaphthalene (1-MN), 2-hexylnaphthalene (2-HN), and NMBB at coal liquefaction conditions. These model species are representative of compound types present in coal and coal liquids. The catalyst precursors were examined individually and combinatorially using several different methods of dispersion: in situ, ex situ, and two-stage processing. The effect of S addition and reaction temperature on the reaction products was also evaluated.

EXPERIMENTAL

Materials. Chemicals used in the HYD and HYC reactions were PYR (99% purity), 1-MN (98% purity), and hexadecane (99% purity) obtained from Aldrich; 2-HN supplied by Dr. M. Farcasiu of the Pittsburgh Energy Technology Center and NMBB obtained from TCI America. The catalyst precursors used in the experiments were iron (III) acetylacetonate (FeAcAc) (15.9% Fe, 99% purity) from Eastman Kodak; iron (III) citrate hydrate (FeCH) (16.7% Fe, 98% purity) from Aldrich; iron (III) naphthenate (FeNaph) (6.0% Fe), iron (III) 2-ethylhexanoate (Fe 2-EH) (8.0 to 11.5% Fe), and iron (III) stearate (FeSTR) (9.0% Fe, 98% purity) from Strem; and molybdenum naphthenate (MoNaph) (6.0% Mo) from Shepherd Chemical. All the model compounds and catalyst precursors were used as received.

Reaction Procedures. Reaction methods used for dispersing the catalysts in the reactions were (1) in situ reaction where the catalyst precursor at a level of 900 to 1100 ppm active metal was added directly into the reaction system and reacted in the presence and absence of S; (2) ex situ reaction where the catalyst precursor reacted in the presence of the model compound was reclaimed, dried for 72 hr in a vacuum oven at 60 °C and reintroduced at a level of 900 to 1100 ppm active metal into a second reaction with PYR; (3) two-stage reaction where the catalyst precursor at a level of 900 to 1100 ppm active metal was added to hexadecane, H_2, and S and reacted for 30 min, then the model species was introduced into the reactor along with H_2 and reacted for another 30 min. The reactions were performed in ~20 cm^3 stainless steel tubular microreactors. Reactions were conducted at 380, 400, or 425 °C for 30 or 60 min with a H_2 pressure of 1250 psig at ambient temperature and an agitation rate of 550 rpm. The solvent used in the reactions was hexadecane; however, because of interference with the analysis of reaction products, NMBB was reacted without a solvent. Reactions were performed both with and without S. When S was added, S was introduced as elemental S in a stoichiometric ratio of 3:1 sulfur:metal, based on the presumption that either Fe_7S_8 or MoS_2 was formed depending on the metal precursor used. Each reaction was at least duplicated; the standard deviations for both HYD and HYC reactions are given in the tables.

Pyrene Hydrogenation. Pyrene HYD reactions were performed using in situ, ex situ, and two-stage reaction methods. Two weight percent PYR in hexadecane was reacted at 380 and 425 °C for the in situ single-stage reactions. In addition, in situ reactions were performed at 380 °C using combined catalysts of Fe-based precursors and MoNaph. The total level of metal was kept constant at 900 to 1100 ppm for each reaction with Fe:Mo weight ratios of 75:25, 50:50, and 25:75 being used. For comparison, reactions with individual catalyst precursors introduced at metal levels of 750, 500, or 250 ppm of the active metal were also performed. Two different types of two-stage reactions were performed with FeNaph and MoNaph combined. In the Type 1 sequence, MoNaph, S, and H_2 were added together in the first stage while FeNaph, PYR, and H_2 were charged in the second stage. In the Type 2 sequence, MoNaph, FeNaph, S, and H_2 were added together in the first stage, and PYR and H_2 were introduced into the second stage. The reaction temperature for both sequences of reactions was 380 °C. The recoveries from the PYR HYD reactions varied but were typically in the range of 85 to 95%.

Hydrocracking Reactions. Hydrocracking reactions using 2 wt % 1-MN or 2-HN in hexadecane were performed at 425 °C for 30 min. 4-(1-Naphthylmethyl)bibenzyl was reacted at 400 °C without solvent for 30 min and 60 min for selected reactions. In situ and two-stage reactions were performed using 1-MN and 2-HN, while in situ reactions were performed using NMBB. In addition, reactions were carried out with combinations of Fe-catalyst precursors and MoNaph. The recoveries of 1-MN and 2-HN were usually in the 80 to 95% range with 2-HN giving the lower recoveries. The recoveries for NMBB were all above 90%.

Analysis. An analysis procedure using UV-visible spectroscopy was developed for measuring the amount of the organometallic complex that reacted under liquefaction conditions. The concentration of Fe or Mo complex present after a given reaction time with hexadecane present in the reactor was determined by UV-visible spectroscopy and was compared to the initial amount of complex introduced. Each Fe complex had to be treated differently in the experimental procedure because of their varying degrees of solubility in hexadecane. Hexadecane was used as the analysis solvent for FeNaph, Fe 2-EH,

and MoNaph; ethanol was the extraction and analysis solvent for FeCH; hot water was used to extract FeAcAc for analysis in ethanol.

Reaction products obtained from the HYD and HYC reactions were analyzed by gas chromatography using a Varian Model 3700 gas chromatograph equipped with FID detection and J&W DB5 30 m column. Quantitation was achieved by employing the internal standard method using p-xylene as the internal standard. The reaction products were identified by comparing retention times with those of authentic compounds and by identifying unknowns by GC-mass spectrometry using a VG70 EHF GC-mass spectrometer.

Definitions. Product slates were determined for each reaction from which the amount of HYD and HYC that occurred was calculated for each species. Percent HYD is defined as the moles of H_2 required to produce the liquid product as a percentage of the moles of H_2 required to hydrogenate the most hydrogenated product. The most hydrogenated liquid product from PYR was considered to be perhydropyrene, from 1-MN, 1-methyldecalin and from 2-HN, 2-hexyldecalin. Percent HYC is defined as the mole percent of the products that have undergone hydrocracking.

RESULTS AND DISCUSSION

Pyrene Hydrogenation Reactions

Pyrene was hydrogenated in the presence of five different slurry-phase Fe catalyst precursors at 380 and 425 °C in the presence and absence of S as presented in Table 1. The activity of the Fe catalyst precursors for PYR HYD was very low in the absence of S but the activity increased when S was added to the system. The hydrogenated products observed using the most active catalyst precursors, FeNaph and FeSTR, in the presence of S, were dihydropyrene (DHP), tetrahydropyrene (THP), and hexahydropyrene (HHP). When S was not present, DHP was the only product formed. The percent HYD obtained with the different Fe systems indicates their degree of activity. Iron naphthenate with S yielded the highest percent HYD at 380 °C giving 12% while at 425 °C FeNaph and FeSTR yielded similar HYD's of 11.5 and 11.9%, respectively. Iron acetylacetonate was the only other Fe catalyst precursor that yielded substantial HYD of 9.3% at 425 °C. Iron citrate hydrate and Fe2-EH yielded low HYD with sulfur at either reaction temperature.

Table 1. Activity of Iron Complexes for Pyrene Hydrogenation[a]

	% Hydrogenation				
	FeNaph	**FeSTR**	**FeCH**	**FeAcAc**	**Fe2-EH**
3:1 S:Fe Ratio					
380°C	12.0±0.3	5.2±0.2	1.0±0.1	0.6±0.1	0.0
425°C	11.5±0.6	11.9±0.4	NP[b]	9.3±0.1	1.4±0.1
No Sulfur					
380°C	0.3±0.0	0.0	0.0	0.2±0.0	0.0
425°C	1.7±0.0	0.0	NP	1.0±0.1	0.8±0.0

[a] Reaction Conditions: 900-1100 ppm of Fe, 30 min, 1250 psig H_2 pressure at ambient conditions, 2 wt % PYR in hexadecane.

[b] NP = not performed.

The solids from the in situ FeNaph reaction with S were analyzed by Mössbauer and XAFS spectroscopy by Dr. G.P. Huffman and Dr. F. E. Huggins of the University of Kentucky. Even though S was present in excess in the reactor, the solids formed were determined to be Fe oxyhydroxide, FeOOH, although a small amount of pyrrhotite might have been formed.[10] The particle size of these solids was less than or equal to 70 Å.[9]

Reactions were also performed with MoNaph with and without S at 380 and 425 °C for 30 min. The presence of S in the reactor allowed the Mo to form finely divided MoS_2.[10,11] The particle size of the MoS_2 was also less than or equal to 70 Å.[9] The finely divided MoS_2 catalyst was an active catalyst for PYR HYD. At 380 °C, the PYR reaction with MoNaph and S yielded 34.6% HYD of PYR with HHP isomers being the primary products as well as a substantial amount of decahydropyrene (DCHP) being formed. When PYR was reacted at 380 °C with MoNaph but without S, 11.7% HYD of PYR occurred with DHP as the primary product and THP as the secondary product. At a higher reaction temperature of 425 °C, the reaction of MoNaph with S resulted in 23.7% HYD of PYR while the reaction without S gave 13.8% HYD. When excess S was present at 425 °C less HYD of PYR occurred. Thermodynamics limited the amount of PYR conversion since PYR was favored at higher reaction temperature.[12] Smaller amounts of partially saturated compounds were produced in the reaction at 425 °C than at 380 °C.

Concentration of Iron Complexes at Liquefaction Conditions. The Fe complexes of FeCH, FeNaph, FeAcAc, and Fe2-EH, each with an initial concentration of 1000 ppm Fe, were reacted at 380 °C with an initial H_2 charge of 1250 psig H_2 introduced at ambient temperature. The concentration of each Fe complex was determined by measuring the visible absorbance at two wavelengths and comparing the absorbance reading with a calibration curve for each complex obtained with the same solvent as was used with the reaction mixture. Each of the Fe complexes disappeared very quickly at liquefaction conditions. After 5 min of reaction, all of the Fe complexes were decomposed; in fact, all of them except FeNaph decomposed after 2 min of reaction. By contrast, MoNaph remained in solution longer; after 10 min of reaction, more than half of the MoNaph remained. However, MoNaph had totally decomposed after 15 min of reaction.

Comparison of Dispersion Methods for the Activity of FeNaph and MoNaph. Three methods of dispersion, in situ, ex situ, and two-stage batch processing, were used to test the effect of dispersion on the catalytic activity of catalysts generated from FeNaph and MoNaph with S. A comparison of the activity of FeNaph and MoNaph for PYR HYD using the in situ method showed that MoNaph plus S resulted in three times as much HYD as did FeNaph plus S. The more highly hydrogenated HHP was the primary product produced with MoNaph while DHP was the primary product from FeNaph. The ex situ method, in which the catalyst produced in an in situ experiment was dried, added to PYR and reacted in a H_2 atmosphere, resulted in much less activity for both FeNaph and MoNaph. The reaction with FeNaph did not convert any PYR while the reaction with MoNaph yielded about half the HYD observed in the in situ reaction.

Two-stage batch reactions were performed in which the catalyst precursor was introduced into hexadecane in the first stage and then reacted in the presence of S and H_2 at 380 °C. After 30 min, the reaction was quenched, gas released, and PYR and a new charge of H_2 were added. The system, including PYR, was then reacted again for 30 min. The two-stage reaction with FeNaph yielded about 6% conversion of PYR to DHP so that its activity was much less than that of the in situ generated catalyst. By contrast, the two-stage reaction with MoNaph yielded higher PYR HYD, 40.2%, compared to 34.6% for the in situ single-stage reaction. Also, substantially more DCHP was formed in the two-stage than in the single-stage in situ reaction. The catalytic activity of MoNaph increased with the two-stage treatment while FeNaph did not.

Effect of Dual Catalysts on Pyrene Hydrogenation. Reactions were performed in which Fe precursors were combined with MoNaph to determine if synergism occurred for PYR HYD. Reactions were performed with 1000 ppm of Fe complex or MoNaph individually and with combinations of ratios of 75:25, 50:50, and 25:75 Fe:Mo with the total active metal loading being 1000 ppm. Results from these reactions in terms of PYR HYD are presented in Table 2.

The dual catalysts of MoNaph with either FeNaph, FeSTR, FeAcAc, or FeCH all showed increased HYD of PYR for at least one combination. FeCH and FeAcAc yielded increased PYR HYD of ~41% at the 250 ppm Fe to 750 ppm Mo ratio compared to 34.6% HYD for 1000 ppm of MoNaph. A direct comparison at equivalent Mo loadings showed that MoNaph reacted individually at 750 ppm only

resulted in 27.8% HYD of PYR. FeSTR combined with MoNaph showed increased HYD of PYR compared to 1000 ppm of MoNaph at ratios of 500 ppm Fe to 500 ppm Mo giving 41.5% HYD and of 250 ppm Fe to 750 ppm Mo, 34.9% HYD. However, if both of these percent values were compared to MoNaph alone at equivalent levels, as shown in Table 2, then substantial increases in percent HYD were obtained. Iron naphthenate combined with MoNaph showed the greatest activity of the dual catalyst systems. At ratios of 750 ppm Fe to 250 ppm Mo and of 500 ppm Fe and 500 ppm Mo, the combination of FeNaph with MoNaph yielded more than 40% HYD of PYR which was more than that which occurred with 1000 ppm Mo and substantially more HYD than occurred with either 250 or 500 ppm of MoNaph.

Table 2. Effect of Combined Catalysts on the Hydrogenation of Pyrene[a]

	1000 ppm Fe	750 ppm Fe 250 ppm Mo	500 ppm Fe 500 ppm Mo	250 ppm Fe 750 ppm Mo	1000 ppm Mo
% Hydrogenation with Mixtures of Fe and Mo Catalyst Precursors					
Fe Naph[b]	12.0±0.3	40.5±1.4	43.6±0.5	32.0±1.0	34.6±1.7
Fe STR	5.2±0.2	26.4±0.8	41.5±0.6	34.9±0.9	34.6±1.7
Fe AcAc	0.6±0.1	3.3±0.2	20.9±0.6	41.8±0.3	34.6±1.7
Fe 2-EH	0.0	7.5±1.0	11.0±1.0	17.1±0.8	34.6±1.7
Fe CH	1.0±0.1	6.3±0.2	29.8±0.3	41.4±0.3	34.6±1.7
% Hydrogenation with Individual Catalyst Precursor					
	1000 ppm	**750 ppm**	**500 ppm**	**250 ppm**	
Fe Naph	12.3±0.3	9.0±0.3	4.7±0.6	3.9±0.3	
Mo Naph	34.6±1.7	27.8±0.3	22.4±0.3	11.7±0.3	

[a] Reaction Conditions: 990-1100 ppm metal, 1250 psig H_2 at ambient temperature, 3:1 S:Fe and S:Mo ratio 380°C, 30 min, 2 wt % PYR in hexadecane.

[b] FeNaph = iron naphthenate; FeSTR = iron stearate; FeAcAc = iron acetylacetonate; Fe2-EH = iron 2-ethylhexanoate; FeCH = iron citrate hydrate; MoNaph = molybdenum naphthenate

Hence, the combined catalysts promoted reactions that increased the HYD of PYR compared to the single catalyst case. The solids obtained from the combined reactions of FeNaph with MoNaph were also analyzed by Mössbauer and XAFS spectroscopy. FeNaph formed $FeSO_4$ in the reaction with combined catalysts while Mo was coordinated with four oxygen atoms.[10] The particle size of both particles was less than or equal to 70 Å.[9] The Fe and Mo catalysts generated from FeNaph and MoNaph, respectively, were present in different forms when both metals were used simultaneously compared to when the individual metals were present in the PYR reactions. These differences may account for the synergism that occurred with both metals being present.

Effect of Two-Stage Processing on Pyrene Hydrogenation. Two-stage PYR HYD reactions were performed using the dual catalysts of FeNaph and MoNaph as presented in Table 3. The dual catalysts were introduced at a total active metal content of 1000 ppm with ratios of 75:25, 50:50, and 25:75 Fe:Mo. The two-stage reactions were performed in two ways: in Type 1 sequence, MoNaph was added to the first stage and FeNaph was added to the second stage; in Type 2 sequence, MoNaph and FeNaph were both added to the first stage. The reactions were also performed with each catalyst precursor individually so that the effect of the dual catalysts on the HYD of PYR could be compared

directly at the given Mo concentration level. All of the reactions with FeNaph reacted individually yielded low levels of PYR HYD.

Comparing the two-stage reactions using the Type 1 sequence to the Type 2 sequence showed that higher levels of HYD of PYR were obtained with Type 1. Increases in HYD were observed using the sequenced catalysts at both 500:500 and 250:750 Fe:Mo ratios compared to the simultaneous addition of catalysts at these combined catalyst loadings. However, the Type 2 reactions resulted in higher levels of HYD at 750:250 Fe:Mo ratio compared to Type 1. Both types resulted in at least two of the ratios having higher HYD of PYR than did the corresponding amount of MoNaph reacted individually.

Ex situ reactions were also performed with the dual catalyst system of FeNaph with MoNaph (Table 3). Almost no HYD of PYR occurred in these reactions. Evidently the removal of the catalyst from the reaction system and subsequent drying of the catalyst resulted in changes either in the catalyst structure or particle size that were detrimental to the HYD activity of the combined catalyst system.

Table 3. Effect of Two-Stage Processing and Ex Situ Reactions on Pyrene Hydrogenation[a]

	% Hydrogenation with Mixtures of FeNaph and MoNaph[c]				
	1000 ppm Fe	750 ppm Fe 250 ppm Mo	500 ppm Fe 500 ppm Mo	250 ppm Fe 750 ppm Mo	1000 ppm Mo
Two-Stage Reaction					
1. Mo added to 1st Stage Fe added to 2nd Stage	0.8±0.1	16.6±0.8	32.8±1.1	30.9±0.9	40.2±0.6
2. Mo & Fe added to 1st Stage	0.8±0.1	23.4±0.4	27.5±0.9	26.9±0.6	40.2±0.6
Ex Situ Reactions	0.0	0.5±0.2	0.8±0.3	NP[b]	18.1±1.1
	% Hydrogenation with Individual Catalyst Precursors				
	1000 ppm	750 ppm	500 ppm	250 ppm	
Two-Stage Reactions					
FeNaph	0.8±0.1	1.6±0.3	1.3±0.2	0.7±0.1	
MoNaph	40.2±0.6	26.4±0.6	17.7±0.4	16.0±0.6	

[a] Reaction Conditions: 250-1000 ppm FeNaph or MoNaph with a total catalyst loading of 1000 ppm, 380°C, 1250 psig H_2 at ambient temperature, 3:1 S:Fe or S:Mo ratio, 30 min, 2 wt% pyrene in hexadecane.

[b] NP = not performed.

[c] FeNaph = iron naphthenate; MoNaph = molybdenum naphthenate.

Hydrocracking Reactions

Reactions were performed in which the HYC activity of selected Fe complexes were tested. The model systems that were used included 1-MN, 2-HN, and NMBB which has been used extensively as model for HYC.[6-8] In each of the reactions, the bond, being tested for HYC was a C-C bond, which was present in different configurations and, hence, bond energies.

Hydrocracking Reactions of 1-Methylnaphthalene and 2-Hexylnaphthalene. The HYC activity of FeNaph and FeSTR for C-C bonds in 1-MN and 2-HN was tested at 425 °C as shown in Table 4. The HYD activity of these Fe catalyst precursors was also evaluated and compared to that obtained with MoNaph. Reactions were performed in situ with the individual and combined catalysts.

Baseline experiments were performed with naphthalene (NAP) to evaluate the effect of any catalytic activity of FeNaph or FeSTR on the aromatic ring structure. When reacted at 425 °C thermally, NAP did not react; however, when FeNaph and FeSTR were introduced with excess S, about 15 mol % tetralin (TET) was formed in the reaction. Only HYD occurred; no HYC of the aromatic ring was

observed. The products observed from 1-MN were primarily the HYD products of 5,6,7,8-tetrahydro-1-methylnaphthalene (5,6,7,8-1-HMN) and 1,2,3,4-tetrahydro-1-methylnaphthalene (1,2,3,4-1-HMN). The hydrocracked product, NAP, was the minor product, present at 2 to 3 mol %. Comparison of the product slate when MoNaph was used showed that substantially more of the hydrogenated products were formed yielding 39% 5,6,7,8-1-HMN and 25% 1,2,3,4-1-HMN, compared to the Fe catalysts where 11-12% 5,6,7,8-HMN and 3.6 to 5.3% 1,2,3,4-1-HMN were formed; however, no NAP was produced. For all of the catalysts, the 5,6,7,8-1-HMN isomer was the preferred product. If 1-methyldecalin is considered to be the most hydrogenated product, then the Fe complexes both yielded between 6 and 7% HYD of 1-MN but less than 3% HYC (Table 4). MoNaph yielded substantially more HYD of 1-MN at ~26%; however, no HYC of the methyl group from the aromatic ring occurred.

Table 4. Comparison of the Activity for the Hydrogenation and Hydrocracking of 1-Methylnaphthalene and 2-Hexylnaphthalene

Product Distribution (mole %)	Catalyst (1000 ppm)						Catalysts (500 ppm)	
	No Catalyst	FeSTR + S	FeNaph + S	MoNaph + S	Two Stage		FeNaph MoNaph + S	MoNaph + S
					FeNaph + S	MoNaph + S		
1-Methylnaphthalene								
% HYD	0.0	6.3±0.4	6.6±0.3	25.8±0.4	5.4±0.6	25.0±0.6	19.0±0.6	13.8±0.8
% HYC	0.0	2.2±0.3	2.7±0.4	0.0	3.5±0.6	2.5±0.6	3.5±0.5	0.0
2-Hexylnaphthalene								
% HYD	0.0	10.4±0.8	14.8±0.7	40.0±1.0	7.0±0.8	38.8±0.9	30.4±1.0	27.7±0.8
% HYC	0.0	9.6±0.2	13.1±0.9	36.4±0.3	6.1±0.3	35.0±1.2	23.7±1.0	25.2±0.4

[a] Reaction Conditions: 900-1100 ppm Fe or Mo, 1250 psig H_2 introduced at ambient temperature; 30 min, 425°C, S:Fe ratio 3:1, S:Mo ratio 3:1, 2 wt% 1-MN or 2-HN in hexadecane

Two-stage processing of FeNaph and MoNaph resulted in more HYC for both catalysts, producing more NAP. In both cases, the percent HYD of the products decreased slightly compared to the single stage in situ reaction. This lesser amount of HYD may have resulted from decreased catalytic activity because of exposure of the catalysts to air between the two stages.

Dual catalysts of FeNaph and MoNaph were combined at 500 ppm each and were reacted with 1-MN. For comparison, a reaction with 500 ppm MoNaph was also performed. The product distribution obtained from the dual catalyst system given in Table 4 showed characteristics of both MoNaph and FeNaph. Fairly high levels of HYD were obtained yielding 19% HYD with 5,6,7,8-1-HMN as the primary HYD product and 1,2,3,4-1-HMN as the secondary one. Hydrocracking also occurred yielding 3.5% HYC with NAP as the product. MoNaph at 500 ppm showed a lesser HYD of 13.8% and no HYC. The dual catalyst for 1-MN enhanced both HYD and HYC.

Hydrocracking of 2-Hexylnaphthalene. The same series of reactions was performed with 2-HN as with 1-MN (Table 4). Products obtained were 2-hexyltetralin (2-HT) and 2-ethyltetralin (2-ET). 2-Hexyltetralin was formed at a slightly higher amount than 2-ET regardless of the catalyst or reaction type. Of the two Fe catalyst precursors, FeNaph was more active for both HYD and HYC in the in situ reactions. However, MoNaph had the most activity yielding 40.0% HYD and 36.4% HYC compared to 14.8% HYD and 13.1% HYC with FeNaph. Two-stage reactions were detrimental to both HYD and HYC of FeNaph; about one-third less of each product was formed than in the in situ single-stage reaction. The reaction of 2-HN with MoNaph also experienced a decrease in the amount of HYD and HYC

occurring, but these decreases were quite small. The dual catalyst system of 500 ppm Fe and 500 ppm Mo resulted in slightly more HYD and slightly less HYC than the reaction with MoNaph at 500 ppm Mo.

Hydrocracking Reactions of 4-(1-Naphthylmethyl)bibenzyl. Reactions were performed using NMBB as a model HYC species for coal. Iron catalyst precursors, FeNaph, FeSTR, and FeAcAc, were reacted with NMBB in the presence and absence of S at 400 °C with no solvent; MoNaph was also used for comparison. All of the catalysts were introduced at an active metal loading of 1000 ppm. The primary products obtained from the reactions of NMBB were methylbibenzyl (MBB), NAP, bibenzyl (BB), and naphthyltolylmethane (NTM). Trace amounts of 1-MN, TET, p-xylene, and toluene were also identified in the reactions products when MoNaph was used.

As has been discussed previously in the literature,[6] NMBB contains five different C-C bond sites, designated as *a, b, c, d,* and *e*, which are susceptible to hydrogenolysis. These bond sites are presented in Figure 1. Products that would be obtained from cleavage at the different bond sites are presented in Table 5. Thermal reactions of NMBB at 400 °C resulted in a small amount of HYC and yielded 1.9 mol % NTM and 3.0 mol% MBB; the percent HYC of the thermal reaction was 4.9±1.3% which indicated a small thermal background. In the catalytic reactions, MBB and NAP were the predominant products.

Hydrocracking reactions were performed thermally, thermally with S, and catalytically with and without S as presented in Table 6. Most reactions were performed for 30 min; however, some of the in situ reactions with individual Fe and Mo precursors with sulfur were also performed for 60 min. The data from these reactions are given in terms of percent HYC which is the sum of the mole percents of all products that were hydrocracked. Percent bond cleavage of *a, b,* and *d* is the sum of the mole percents of those reaction products that were produced from cleavage of *a, b,* and *d*. Selectivity is defined as the cleavage of a given bond divided by the sum of the cleavage of bonds *a, b,* and *d*.

Figure 1. Cleavage Sites for 4-(1-Naphthylmethyl)bibenzyl.

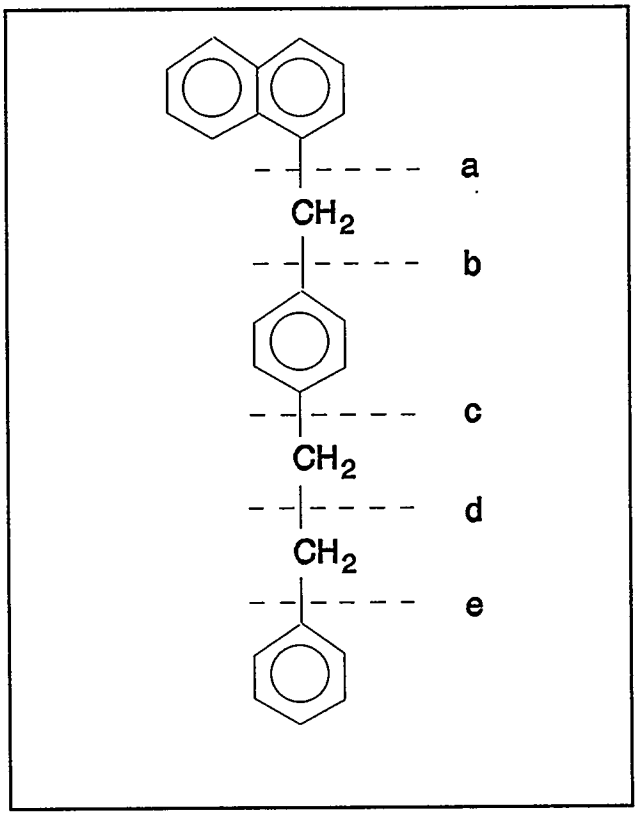

Table 5. Possible Products from the Hydrocracking Reactions of 4-(1-Naphthylmethyl)bibenzyl

Bound Cleaved	Products Observed	Reaction Pathways
a	Methylbibenzyl, Naphthalene, Tetralin	1
b	Methylnaphthalene, Bibenzyl	2
c	Benzylnaphthalene, Ethylbenzene	3
d	Naphthyltolylmethane, Toluene	4
e	Naphthyltolylethane, Benzene	5

Table 6. Selectivity of Iron and Molybdenum Catalysts for Hydrocracking 4-(1-Naphthylmethyl)bibenzyl

Catalyst Precursor	Reaction Time (min)	HYC (%)	Cleavage of $a+b+d$ (%)	Selectivity x 100%		
				$\frac{a}{(a+b+d)}$	$\frac{a+b}{a+b+d}$	$\frac{d}{(a+b+d)}$
Thermal	30	4.9±1.3	4.9	61	61	39
Sulfur	30	9.3±2.7	7.3	64	67	33
FeNaph	30	5.5±1.0	4.6	74	74	26
FeNaph+S	30	13.5±1.4	10.4	79	86	14
FeAcAc+S	30	5.7±1.4	5.0	82	82	18
FeSTR+S	30	6.0±1.5	4.7	68	79	21
MoNaph	30	6.4±0.9	5.3	72	72	28
MoNaph+S[a]	30	28.5±2.1	21.0	87	94	6
MoNaph+S[b]	30	39.4±2.3	27.5	89	96	4
FeSTR+MoNaph+S[c]	30	8.9±1.4	6.7	69	81	19
FeNaph+MoNaph+S[c]	30	22.9±1.6	17.9	86	90	10
FeAcAc+MoNaph+S[d]	30	18.1±1.8	13.9	92	92	8
FeNaph+S	60	18.7±2.2	12.1	69	69	31
FeAcAc+S	60	9.9±2.0	6.4	56	56	44
FeSTR+S	60	7.8±1.5	5.2	62	62	38
MoNaph+S	60	47.3±3.8	34.8	89	95	5

[a] 500 ppm Mo
[b] 1000 ppm Mo
[c] 500 ppm Fe + 500 ppm Mo
[d] 250 ppm Fe + 750 ppm Mo

The thermal reaction showed a background HYC of 4.9% while the introduction of S nearly doubled the amount of HYC to 9.3%. The introduction of FeNaph and MoNaph without S resulted in low HYC of 5.5 and 6.0%, respectively. Addition of S increased the HYC from FeNaph to 13.5%. The other two Fe catalyst precursors used, FeAcAc and FeSTR, reacted with S gave low HYC of 5.7 and 6.0%, respectively. Increasing the reaction time to 60 min increased the amount of HYC observed for all three Fe catalyst precursors when reacted with S. The largest increase was observed with FeNaph, which increased from 13.5 to 18.7% HYC.

The percent HYC of NMBB with MoNaph and S at both 500 and 1000 ppm Mo resulted in substantial HYC of 28.5 and 39.4%, respectively; however, only trace amounts of HYD occurred. Increased reaction time of 60 min resulted in an increased HYC of 47.3%. Combinations of MoNaph with either

FeNaph and FeSTR at 500 ppm of each active metal catalyst and FeAcAc at 250 ppm Fe and 750 ppm Mo produced an increased HYC compared to the specific Fe catalyst. Iron naphthenate and FeAcAc showed the largest increases while FeSTR showed only a small increase. By contrast, if the percent HYC that occurred in the combined reactions is compared to that of MoNaph at the same loading level the percent HYC decreased. The largest decrease was observed for the reaction of FeSTR combined with MoNaph. Hence, the presence of the iron species in the reaction was detrimental to the HYC activity of MoNaph.

The percent HYC that has been discussed involved HYC of all C-C bonds observed during the reaction with the different catalyst precursors. The bond cleavage also given in the table is the addition of the mole percent of cleavage that occurred at sites *a, b,* and *d*. In every reaction except the thermal reaction without S, the sum of the cleavage at *a, b*, and *d* was less than the total HYC that occurred in the reaction.

The selectivity for HYC of NMBB at the two primary sites of cleavage *a* and *d* is shown in Table 6. For the 30 min reactions, the thermal reactions with and without S showed the lowest selectivity for cleavage at site *a* in the low 60% range. The reactions with iron precursors showed intermediate selectivity between 68 and 82%. Molybdenum naphthenate with S had the highest selectivity for cleavage at site *a* yielding 87 and 89% at 500 and 1000 ppm, respectively. Combining Fe precursors with MoNaph increased the selectivity for *a* to varying degrees for the different Fe species. The Fe precursors when reacted for a longer time of 60 min showed a decreased selectivity for *a* and a substantial increase in the selectivity for *d*. By contrast, the selectivity of MoNaph did not change with the increased reaction time.

The selectivity for cleavage appears to be dependent upon the reaction conditions and catalyst used. The selectivity for cleavage at sites *a+b* was less in the work performed by Farcasiu and Smith[8] than in this study. For comparison the selectivity defined as *a+b* divided by the sum of *a+b+d* for the reactions performed in this study is also given in Table 6. Although the reaction temperatures were similar, the source of H_2 was different in the two sets of reactions; a H_2 donor was the source H_2 used by Farcasiu and Smith,[8] while molecular H_2 at ~19 MPa was the source in this work. The catalyst form and particle size present in the reactor were also most likely different.

The primary factors that affected the selectivity for specific bond cleavage of C-C bonds in NMBB at these reaction conditions were (1) the presence or absence of a catalyst; (2) the type of active metal present in the catalyst; (3) the activity of catalyst generated in situ; (4) the presence or absence of S; and (5) reaction time. These same factors also strongly affected the amount of cleavage of bonds *a, b*, and *d* as well as the percent HYC.

SUMMARY

The activity of slurry-phase Fe-based catalysts for HYD of PYR was enhanced by the presence of S and higher reaction temperature. Of the five Fe precursors tested, FeNaph and FeSTR were the most active for hydrogenating PYR. The method of catalyst introduction affected the reactivity of the finely dispersed catalyst. Introducing the catalyst precursor directly into the reaction mixture was the most effective. Molybdenum naphthenate, used as a bench mark for catalytic activity, gave increased conversion and more highly saturated products of PYR compared to that achieved by the Fe catalysts. Combinations of MoNaph with the different Fe catalyst showed substantial increases in PYR HYD except for one Fe precursor. The practical value of using these combined catalysts is that more activity was achieved with a lesser amount of the more expensive Mo metal. The amount of HYC C-C bonds effected by the finely divided Fe catalyst generated in situ was different than that achieved by MoS_2 generated in situ. The finely divided Fe catalysts were not nearly as active as the finely divided MoS_2 and also had different selectivities for bond cleavage.

ACKNOWLEDGEMENTS

The support of the United States Department of Energy through the Consortium for Fossil Fuel Liquefaction Science under Contract No. UKRF-4-24351-90-84 is gratefully acknowledged. The analysis of several of the catalysts generated in this research by Dr. G. P. Huffman and Dr. F. Huggins of the University

of Kentucky is also gratefully acknowledged. The donation of 2-hexylnaphthalene by Dr. M. Farcasiu of the United States Department of Energy is sincerely appreciated.

REFERENCES

1. Kim, H.; Curtis, C.W. *Am. Chem. Soc. Fuel Chem. Div. Prepr.*, 35(4)1064-1070, 1990.
2. Pellegrino, J.L.; Curtis, C.W. *Energy and Fuels,* 3(2)160-168, 1989.
3. *Cooperative Research in Coal Liquefaction.* Annual Report (5/1/90-4/30/91) on DOE Contract No. DE-FC22-89PC89851, February 15, 1992.
4. Pradhan, V.R.; Herrick, D.E.; Tierney, J.W.; Wender, I. *Energy and Fuels,* 5(5)712-720, 1991.
5. Suzuki, T.; Yamada, H.; Sears, P.L.; Watanabe, Y. *Energy and Fuels, 3,* 707-713, 1989.
6. Farcasiu, M., Smith, C.M.; Pradhan, V.R., Wender, I. *Fuel Proc. Tech., 29,* 199-208, 1991.
7. Farcasiu, M.; Smith, C.M. *Am. Chem. Soc. Fuel Chem. Div. Prepr., 35,* 404-413, 1990.
8. Farcasiu, M.; Smith, C.M. *Energy and Fuels, 5,* 83-87, 1991.
9. Huffman, G.P.; Ganguly, B.; Zhao, J.; Rao, K.R.P.; Shah, N.; Feng, Z.; Huggins, F.E.; Taghiei, M.M.; Lu, F.; Wender, I.; Pradhan, V.R.; Tierney, J.W.; Seehra, M.S.; Ibrahim, M.M.; Shabtai, J., Eyring, E.M. *Energy and Fuels, 7,* 285-296, 1993.
10. Personal communication, Dr. G. P. Huffman and Dr. F. E. Huggins, 1993.
11. Kim, H.; Curtis, C.W.; Cronauer, D.C.; Sajkowski, D.J. *Amer. Chem. Soc. Fuel Chem. Div. Prepr.*, 34(4)1431-1438, 1989.
12. Ting, P.S.; Curtis, C.W.; Cronauer, D.C. *Energy and Fuels, 6,* 511-518, 1992.

NOMENCLATURE

1,2,3,4-1-HMN	=	1,2,3,4-tetrahydro-1-methylnaphthalene
1-MN	=	1-methylnaphthalene
2-ET	=	2-ethyltetralin
2-HN	=	2-hexylnaphthalene
2-HT	=	2-hexyltetralin
5,6,7,8-1-HMN	=	5,6,7,8-tetrahydro-1-methylnaphthalene
% HYC	=	percent hydrocracking
% HYD	=	percent hydrogenation
BB	=	bibenzyl
DCHP	=	decahydropyrene
DHP	=	dihydropyrene
Fe2-EH	=	iron 2-ethylhexanoate
FeAcAc	=	iron acetylacetonate
FeCH	=	iron citrate hydrate
FeNaph	=	iron naphthenate
FeSTR	=	iron stearate
HHP	=	hexahydropyrene
MBB	=	methylbibenzyl
MoNaph	=	molybdenum naphthenate
NAP	=	naphthalene
NMBB	=	4-(1-naphthylmethyl) bibenzyl
NTM	=	naphthyltolylmethane
PYR	=	pyrene
TET	=	tetralin
THP	=	tetrahydropyrene
XAFS	=	X-ray absorption fine structure

Task II

Exploratory Research on Coal Conversion

Program Coordinators: Henk Meuzelaar and Mohindar Seehra

TASK II

Project II.1

COAL STRUCTURE/LIQUEFACTION YIELD CORRELATION BY MEANS OF ADVANCED NMR TECHNIQUES

Ronald J. Pugmire
University of Utah

During the period of May 1, 1992 to April 30, 1993, our efforts focused on the development and testing of a number of techniques that can provide chemical shift information on polycyclic aromatic hydrocarbons, which serve as models of the structural features in the aromatic clusters found in coal. Obtaining the principal components of the chemical shift tensor for compounds with more than four distinct carbons using the standard static solid NMR techniques is often impossible due to overlap of the shielding patterns of each of the carbons. However, there have been many techniques developed to isolate the lineshape of a single carbon from the remaining carbons, either by separating the individual patterns in a two dimensional space or selectively observing only one carbon.

We recently published a paper on the application of variable angle sample spinning (VASS) technique to a series of substituted naphthalenes,[1] each with three different aromatic shift tensors. This work was also the focus of a talk presented at the International Conference on Coal Science in England during August 1991. A second paper, "Selective Saturation and Inversion of Multiple Resonances in High Resolution Solid State ^{13}C Experiments using Slow Spinning CP/MAS and Tailored DANTE Pulse Sequence", was recently published.[2] This experiment employs rapid spinning of a solid sample at the magic angle. The chemical shift anisotropy (CSA) of each distinct carbon in a sample collapses into a relatively narrow line at the isotropic or average chemical shift. If the spinning speed is less than the width of the

shift pattern (the slow MAS condition) one does not obtain a single line but rather, one obtains a group of lines spaced about the central isotropic line at the interval of the spinning speed. By simulating the intensity pattern of this spinning sideband family, the components of the tensor can be retrieved. It is possible to isolate a shift pattern from only one carbon by selectively saturating the signals due to the remaining carbons in the sample. This has been done in the past; however, literature examples are limited to cases where only one or two resonances are either saturated or inverted.[3] By taking advantage of the long ^{13}C T_1' values commonly encountered in solids, one can selectively saturate a number of resonances by sequentially applying several DANTE pulse sequences centered at different frequency offsets. In addition, it has been demonstrated that if one sideband of a spinning sideband family is selectively saturated the entire family is saturated.[4] Therefore, a spectrum of only one or two families of spinning sidebands can be isolated from a sample that contains a number of resonances.

A probe to perform the magic angle hopping experiment, developed by Bax and Maciel in 1983,[5] has been built in our laboratory. The magic angle hopping experiment separates the individual isotropic chemical shift patterns in a second dimension of a spectrum, removing overlap. By looking at slices in the 2-D space, individual shift patterns are obtained, making the retrieval of the tensor components simple. In the case of magic angle hopping, a static sample, held at the magic angle, is quickly jumped between three orientations 120° apart such that the sample spends one-third of its time at each position. This has the same averaging effect on the CSA as rapidly spinning at the magic angle. A static NMR probe coupled with a motor and encoder was assembled in our laboratory to rotate the sample between the three positions when a signal is received from the spectrometer.

The original magic angle hopping experiment has several shortcomings, preventing its

widespread use. A major problem was obtaining a motor to hop the sample very quickly, in a time short in comparison the spin lattice relaxation time of the sample. In addition, the original pulse sequence was phase modulated requiring the spectrum to be obtained in an obsolete mode intensity, leading to poor resolution in the second dimension.

In our laboratory we have used the same motor system and controller used in the commercial DAS system, which allows for each hop to be completed in less than 60 ms, compared to the 150 ms time reported in the Bax and Maciel paper. In addition, the experiment was modified to obtain the data in a hypercomplex manner (the techniques to do this were developed after 1983 for use in 2-D liquid NMR spectroscopic methods) in order to obtain a pure absorption mode spectrum, resulting in better resolution. These changes in the pulse sequence also lead to a gain in signal to noise over the previous experiment.[6]

A new experiment based on that developed by Z. Gan[7] has been implemented in our laboratory. In Gan's experiment[7] the hopping between the three positions is replaced by continuous spinning at the magic angle at a relatively low rate (in the range of 100 Hz). The evolution time of this 2-D technique is then divided into three segments, each consisting of one-third of a rotor cycle. Between these segments the prepared magnetization is stored along the magnetic field after evolving for one-third of the evolution time. As the evolution time is about an order of magnitude less than the time it takes the rotor to rotate 120°, the sample is essentially static during this evolution time.

The chemical shift, which is the sum of the isotropic and the CSA contribution, is different during each of these segments. However, the average of the chemical shift over the entire sequence is again only the isotropic chemical shift due to the fact that the chemical shift is a second rank tensor. The resulting 2-D spectrum is identical to that obtained in the magic angle hopping experiment. The advantage of this new method, however, is that the

need to mechanically hop the sample is removed. This experiment can be done on any magic angle spinning probe as long as a constant slow speed can be maintained. However, since most spinning systems are built for high speeds and are not stable enough for this experiment at lower speeds, this slow turning experiment can be difficult to perform on standard MAS probes since a very slight variation in the air pressure corresponds to a large change in the rotor spinning speed.

In our laboratory a very large volume (about 6 cm^3) rotor system and a probe has been constructed. The maximum spinning speed of this system is several hundred Hz, and its speed is very constant (± 1 Hz) over 24 hours, the length of time needed for a typical experiment. In addition, the large sample volume allows for good signal to noise to be obtained in a relatively short time for a 2-D experiment.

Two important variations of the Gan experiment have been developed in our laboratory. The first, referred to as the "5 π pulse" experiment[8] employs a constant evolution time synchronized to the rotor period during which 5 π pulses are applied. This two-dimensional experiment yields isotropic chemical shifts in the evolution dimension and undistorted slow-spinning-sideband chemical shift anisotropy powder patterns in the acquisition dimension. Peaks separated by only 1.07 ppm in 1,2,3-trimethoxybenzene are clearly resolved with this experiment.[8] The success of the constant-time method would require that the spin system have relatively long T_2 values, but when this condition obtains the magnetization is used more effectively.

We have noted, however, that the Gan and 5-π pulse experiment produce spectral artifacts in the form of baseline distortions. We have therefore developed a 3-π pulse sequence (which we now call the Magic Angle Turning, MAT, experiment) which significantly improves the baseline. The pulse sequence employed by Gan is shown in Figure

III.2.1c. The 2D contour plot for 1,2,3-trimethoxybenzene (1,2,3-TMB) is shown in Figure III.2.2 together with the projection of the isotropic shifts onto the isotropic chemical shift axis. Note the baseline distortion in Figure III.2.2b. The 3-p MAT pulse sequence (Figure III.2.1a) was used to acquire the 2D contour plot of 1,2,3-TMB shown in Figure III.2.3a. The isotropic chemical shift projections (Figure III.2.3b) exhibit none of the baseline distortions seen in Figure III.2.2b. The resultant powder pattern for each carbon is seen in Figure III.2.3c. Variations of the basic 3-p MAT experiment can be used to suppress protonated carbons (dipolar dephasing, Figure III.2.1b) and display only protonated carbons (short contact time experiments) as seen in Figures III.2.4 and III.2.5.

The MAT experiment has been applied to coals and the spectra of Pocahontas coal (Argonne Premium Sample Bank) are shown in Figure III.2.6. In Figure III.2.7, the slices taken at various isotropic shift values illustrate the power of the MAT experiment in identifying carbons of various types by means of the CSA. The resultant CSA powder patterns along with the results obtained from the short contact time and the dipolar dephasing experiments are shown in Figure III.2.7. It is obvious that the overlapping of the powder patterns (Figure III.2.7b) of the protonated and nonprotonated aromatic carbons are successfully separated by the short contact time (Figure III.2.7c) experiment and the dipolar dephasing experiment (Figure III.2.7d).

Similar data have been obtained on all of the Argonne Premium Coal Samples. The aromaticity, f_a, obtained with the MAT experiment correlate very well with the data of Solum, et al.[9] (see Table III.2.1).

To summarize, we now possess the capability in our laboratory to obtain the chemical shift tensor components in solids by several different 2-D methods. These 2-D methods greatly expand the molecules that are feasible to study, as we are no longer limited to looking

at only smaller aromatic systems with high degrees of symmetry in order to have only three or four magnetically inequivalent carbons. In particular, the 3-π MAT experiment looks very promising. We have successfully demonstrated that this experiment can be utilized for coal studies and we will shortly undertake a detailed analysis of the data that can be obtained with this new experimental technique.

REFERENCES

1. A.M. Orendt, N.K. Sethi, J.C. Facelli, W.J. Horton, R.J. Pugmire, and D.M. Grant, *J. Am. Chem. Soc.*, 114 (1992) 2832.

2. J.Z. Hu, R.J. Pugmire, A.M. Orendt, D.M. Grant, and C. Ye, *Solid State NMR*, 1992, 1, 185.

3. H. Geen, X.-L. Wu, P. Xu, J. Friedrich, R. Freeman, *J. Magn. Reson.*, 81 (1989) 206.

4. P. Carvatti, G. Bodenhausen, R.R. Ernst, *J. Magn. Reson.*, 55 (1983) 88.

5. A. Bax, N.M. Szeverenyi, G.E. Maciel, *J. Magn. Reson.*, 55 (1983) 147.

6. J.Z. Hu, A.M. Orendt, D.W. Alderman, C. Ye, R.J. Pugmire, and D.M. Grant, *Solid State NMR*, 1993, in press.

7. Z. Gan, J. Am. Chem. Soc., 1992, 114, 8307; *J. Magn. Reson.*, (1992).

8. J.Z. Hu, D.W. Alderman, C. Ye, R.J. Pugmire, and D.M. Grant, *J. Magn. Reson.*, 1993, in press.

9. M.S. Solum, R.J. Pugmire, and D.M. Grant, *Energy & Fuels*, 1989, 3, 187.

Table III.2.1
Aromaticities of Argonne Premium Coals
Obtained by the MAT Experiment

Coal	f_a (by MAT)	f_a (by CP/MAS)[a]
Pocahontas	0.86	0.86
Upper-Freeport	0.80	0.81
Stockton	0.73	0.75
Pittsburgh #8	0.75	0.72
Illinois #6	0.72	0.72
Blind Canyon	0.64	0.65
North Dakota Zap	0.67	0.65
Wyodak	0.62	0.63

a. Reference 9

Figure III.2.1. The pulse sequences for the magic angle turning (MAT) experiment. τ is any integral number of rotor periods (except a multiple of three rotor periods). During the measurement, one rotor period was used.

a) the 3-π MAT pulse sequence.

b) the dipolar dephased 3-π MAT pulse sequence.

c) the original MAT pulse sequence used by Gan where D is a time period determined by probe ring-down and receiver recovery.

Figure III.2.2. a) The 2D contour plot spectrum of 1,2,3-TMB obtained using the original MAT pulse sequence in Figure III.2.1c at a sample spinning rate of 44±0.025Hz. The dead time Δ is found to be 30 μs in this system. No line broadening was applied in either dimension. This spectrum was acquired using the following parameters: contact time 4 ms, recycle delay 8 s, t_1 increment 120 μs (three times the acquisition dimension), 110 increments acquired with 64 scans in each increment (i.e., 32 scans in each of the real and the imaginary FID for that t_1 time). Total experiment time was about 16 hours. The decoupler offset was set to the middle of the aromatic proton chemical shifts in order to improve the lineshape of the protonated aromatic carbons. b) the isotropic chemical shift spectrum which is the summed projection of the data onto the isotropic chemical shift axis.

Figure III.2.3. a) The 2D contour plot spectrum of 1,2,3-TMB obtained using the 3-π MAT pulse sequence in Figure III.2.2a at a sample spinning rate of 44±0.025Hz. The experimental parameters are the same as those for Figure III.2.2 except 140 increment was used and the total experiment time is about 20 hours. The time period Δ is chosen as 60 μs. No line broadening was applied in either dimension. b) the isotropic chemical shift spectrum obtained from a. c) the resultant powder pattern for each carbon.

Figure III.2.4. a) The isotropic chemical shift projection spectrum for 1,2,3-TMB obtained by using the dipolar dephasing 3-π MAT pulse sequence in Figure III.2.2b with a dephasing time of 2^*DD=60 μs and p_3-4ms. The other experimental parameters are the same as those for Figure III.2.4. b) the resultant powder patterns for the nonprotonated aromatic as well as the methoxy carbons.

Figure III.2.5. a) The isotropic chemical shift projection spectrum for 1,2,3-TMB obtained by using the 3-π MAT sequence with a short contact time of 60 μs.

Figure III.2.6. a) The 2D contour plot spectrum of Pocahontas coal obtained using the 3-π MAT pulse sequence at a sample spinning rate of 44±0.025Hz with Δ chosen as 60 μs. No line broadening was applied in both dimensions. The experimental parameters are: contact time 2 ms, recycle delay 2s, t_1 increment of 93.75 μs with 25 increment acquired, 512 scans per complex pair. The total measuring time is about 8 hours. b) the isotropic chemical shift spectrum.

Figure III.2.7. The powder patterns for several selected isotropic chemical shift positions in Pocahontas coal obtained by different MAT techniques. (a) and (b) were obtained from Figure III.2.6. (c) was obtained from a short contact time 3-π MAT experiment with a contact time of 50 μs. (d) and (e) were obtained from a dipolar dephasing 3-π MAT experiment with a dipolar dephasing periods of 2^*DD=60 μs and p_3=1.5ms.

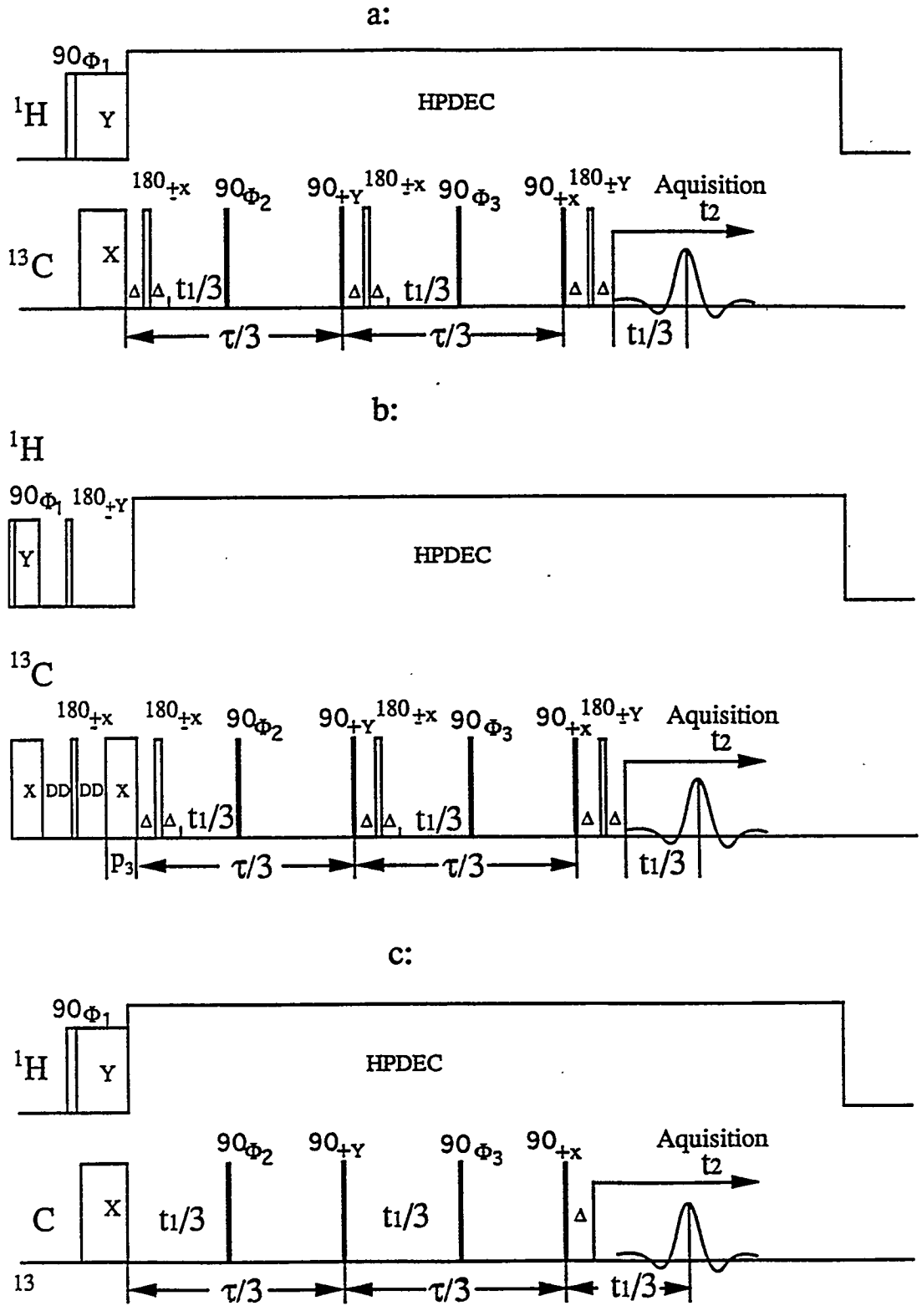

Figure III.2.1. The pulse sequences for the magic angle turning (MAT) experiment. τ is any integral number of rotor periods (except a multiple of three rotor periods). During the measurement, one rotor period was used.

a) the 3-π MAT pulse sequence.

b) the dipolar dephased 3-π MAT pulse sequence.

c) the original MAT pulse sequence used by Gan where Δ is a time period determined by probe ring-down and receiver recovery.

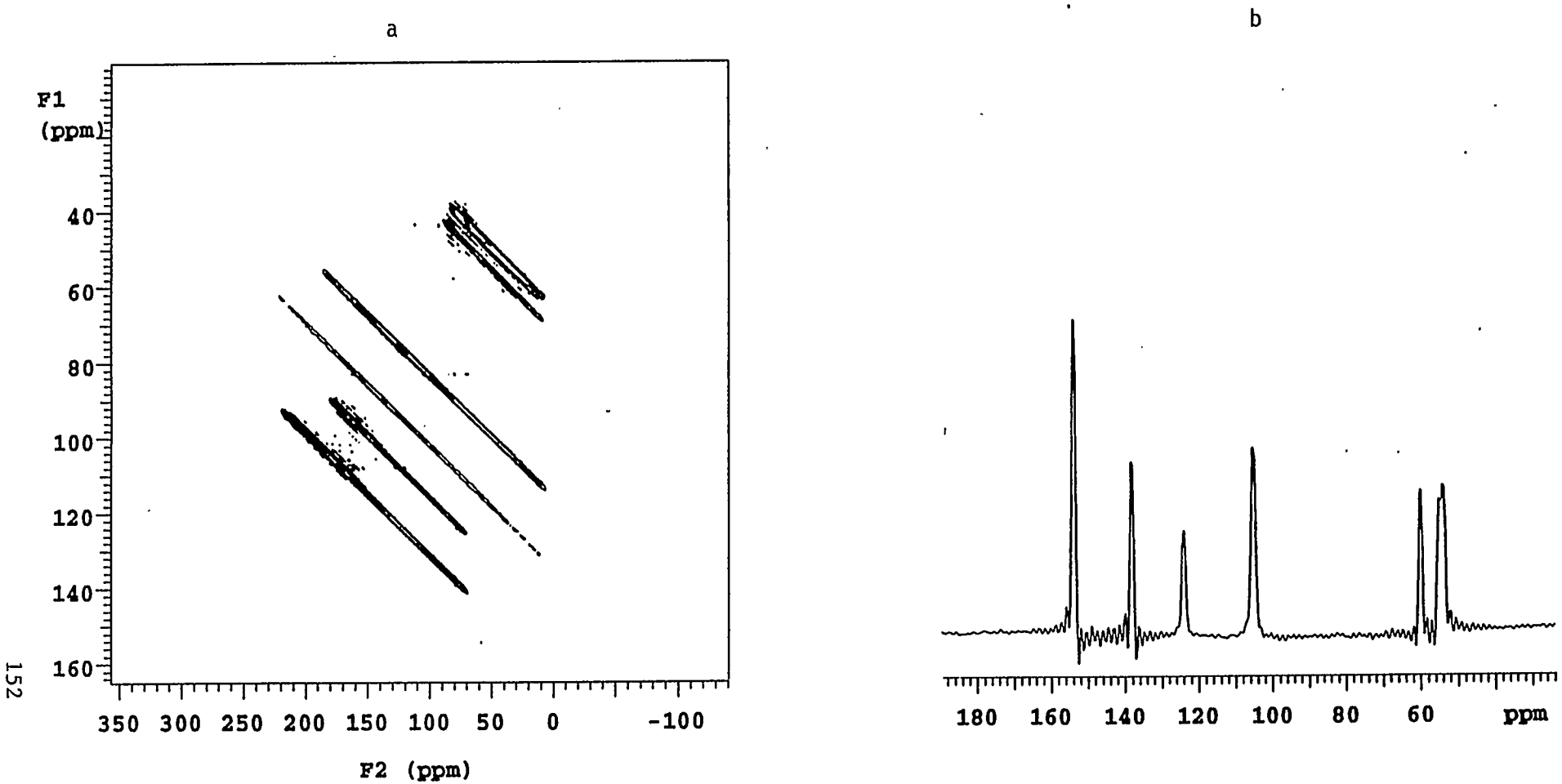

Figure III.2.2. a) The 2D contour plot spectrum of 1,2,3-TMB obtained using the original MAT pulse sequence in Figure 1c at a sample spinning rate of 44±0.025Hz. The dead time Δ is found to be 30μs in this system. No line broadening was applied in either dimension. This spectrum was acquired using the following parameters: contact time 4ms, recycle delay 8s, t_1 increment 120μs (three times the acquisition dimension), 110 increments acquired with 64 scans in each increment (i.e., 32 scans in each of the real and the imaginary FID for that t_1 time). Total experiment time was about 16 hours. The decoupler offset was set to the middle of the aromatic proton chemical shifts in order to improve the lineshape of the protonated aromatic carbons.
b) the isotropic chemical shift spectrum which is the summed projection of the data onto the isotropic chemical shift axis.

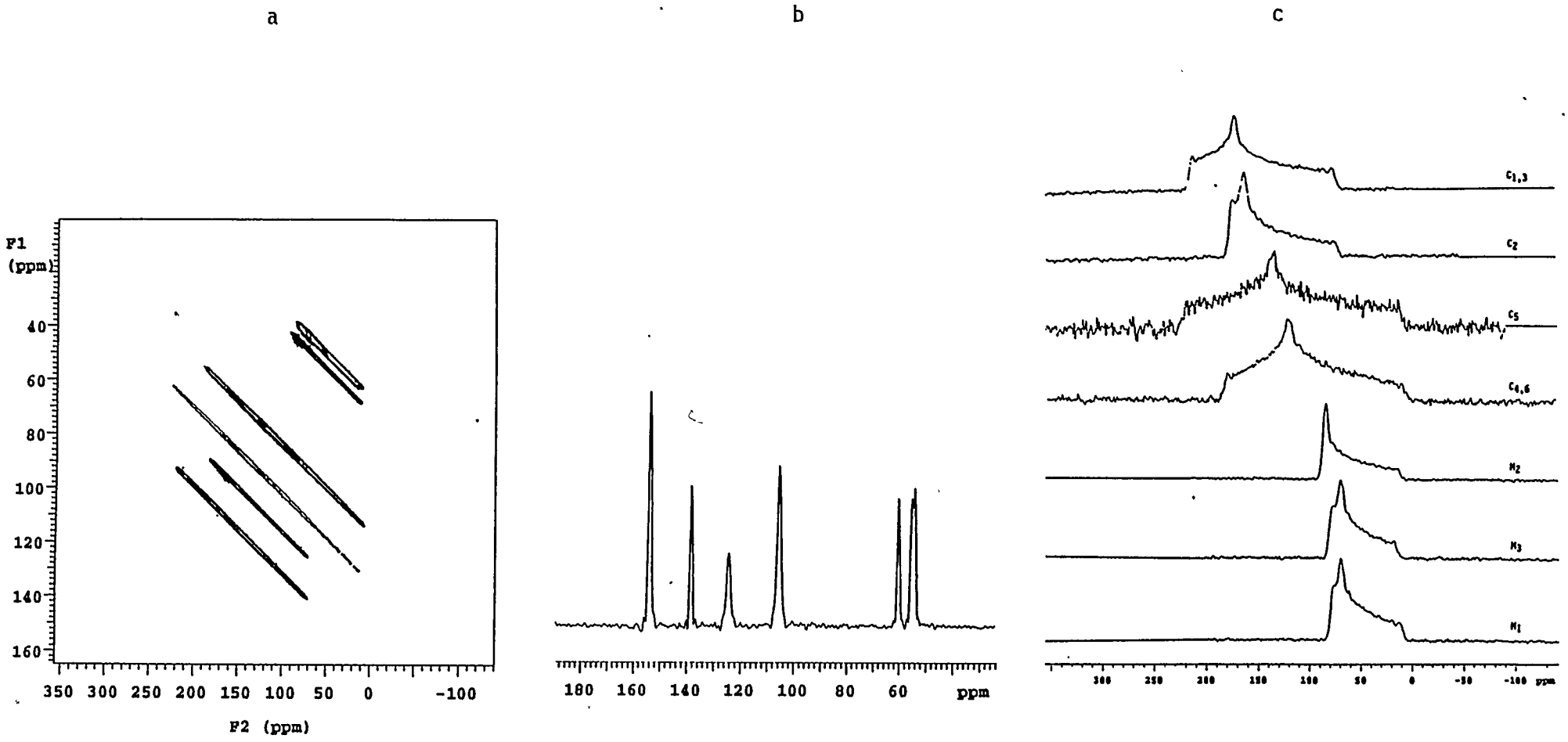

Figure III.2.3. a) The 2D contour plot spectrum of 1,2,3-TMB obtained using the 3-π MAT pulse sequence in Figure 2a at a sample spinning rate of 44±0.025Hz. The experimental parameters are the same as those for Figure 2 except 140 increment was used and the total experiment time is about 20 hours. The time period Δ is chosen as 60μs. No line broadening was applied in either dimension.
b) the isotropic chemical shift spectrum obtained from a.
c) the resultant powder pattern for each carbon.

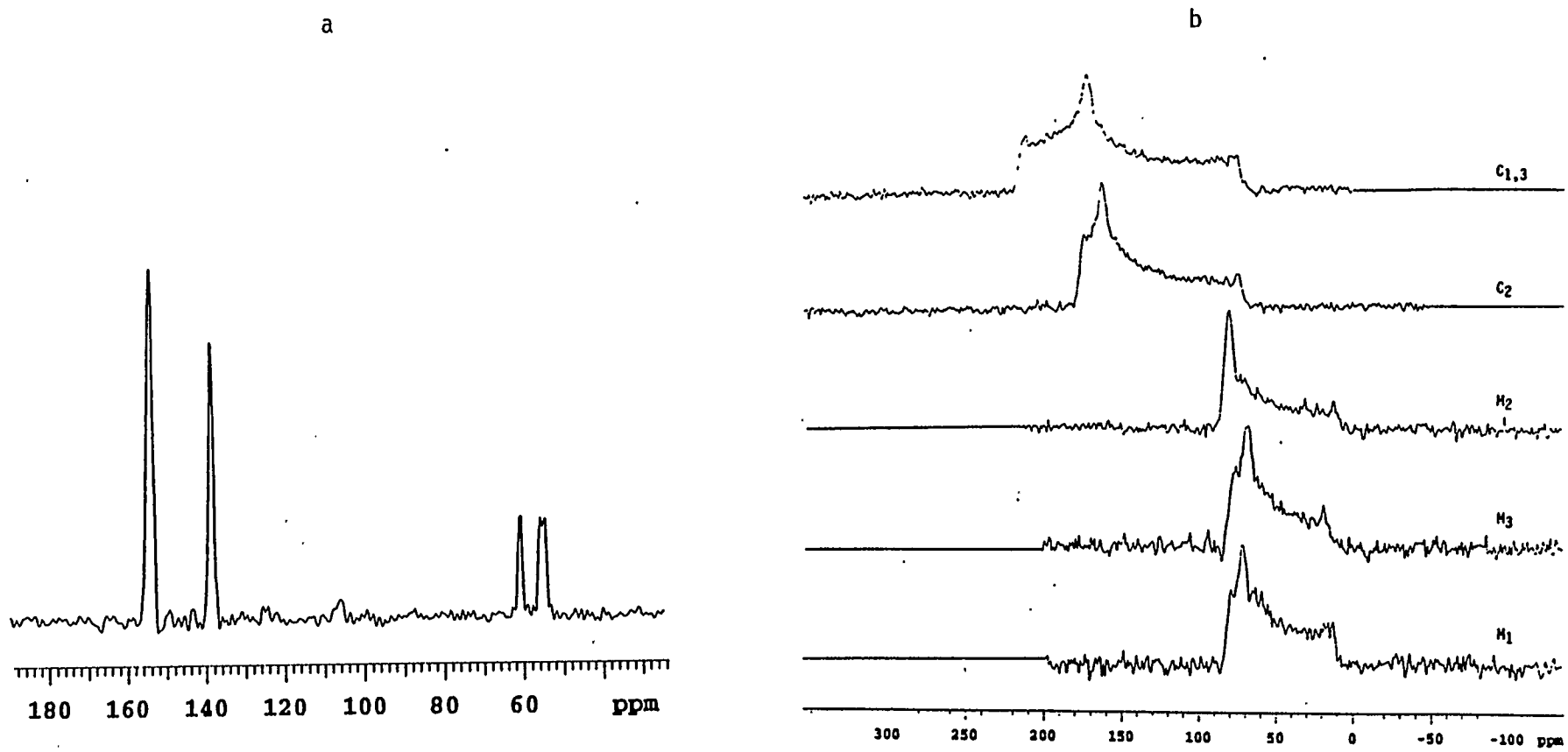

Figure III.2.4. a) The isotropic chemical shift projection spectrum for 1,2,3-TMB obtained by using the dipolar dephasing 3-π MAT pulse sequence in Figure 2b with a dephasing time of $2^{*}DD=60\mu s$ and p_3-4ms. The other experimental parameters are the same as those for Figure 4.
b) the resultant powder patterns for the nonprotonated aromatic as well as the methoxy carbons.

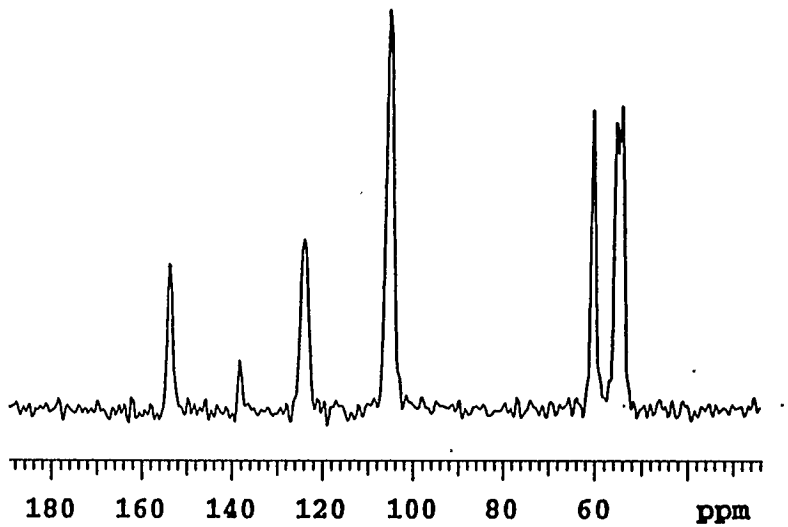

Figure III.2.5. a) The isotropic chemical shift projection spectrum for 1,2,3-TMB obtained by using the 3-π MAT sequence with a short contact time of 60μs.

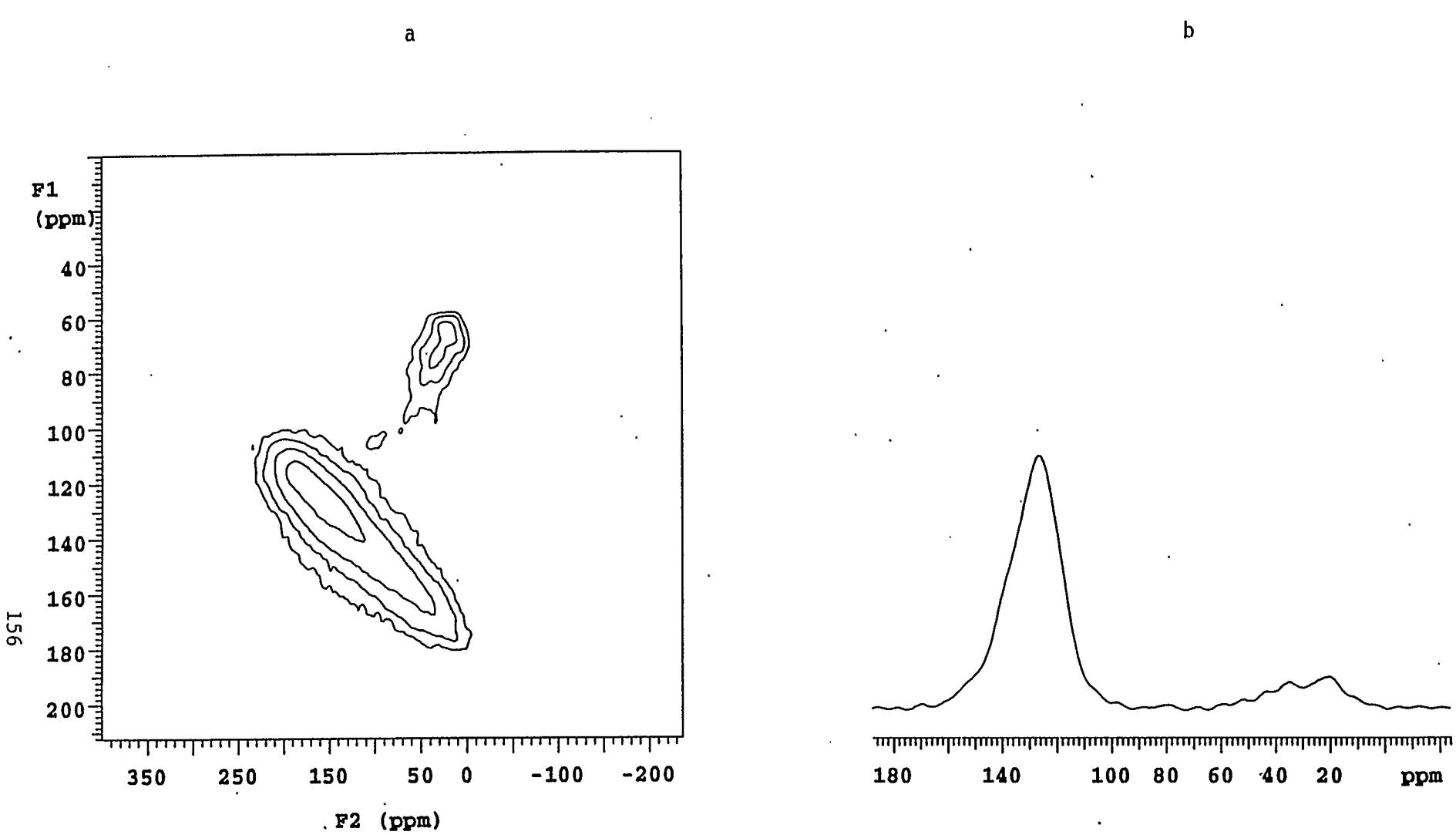

Figure III.2.6. a) The 2D contour plot spectrum of Pocahontas coal obtained using the 3-π MAT pulse sequence at a sample spinning rate of 44±0.025Hz with Δ chosen as 60 μs. No line broadening was applied in both dimensions. The experimental parameters are: contact time 2 ms, recycle delay 2s, t_1 increment of 93.75μs with 25 increment acquired, 512 scans per complex pair. The total measuring time is about 8 hours.
b) the isotropic chemical shift spectrum.

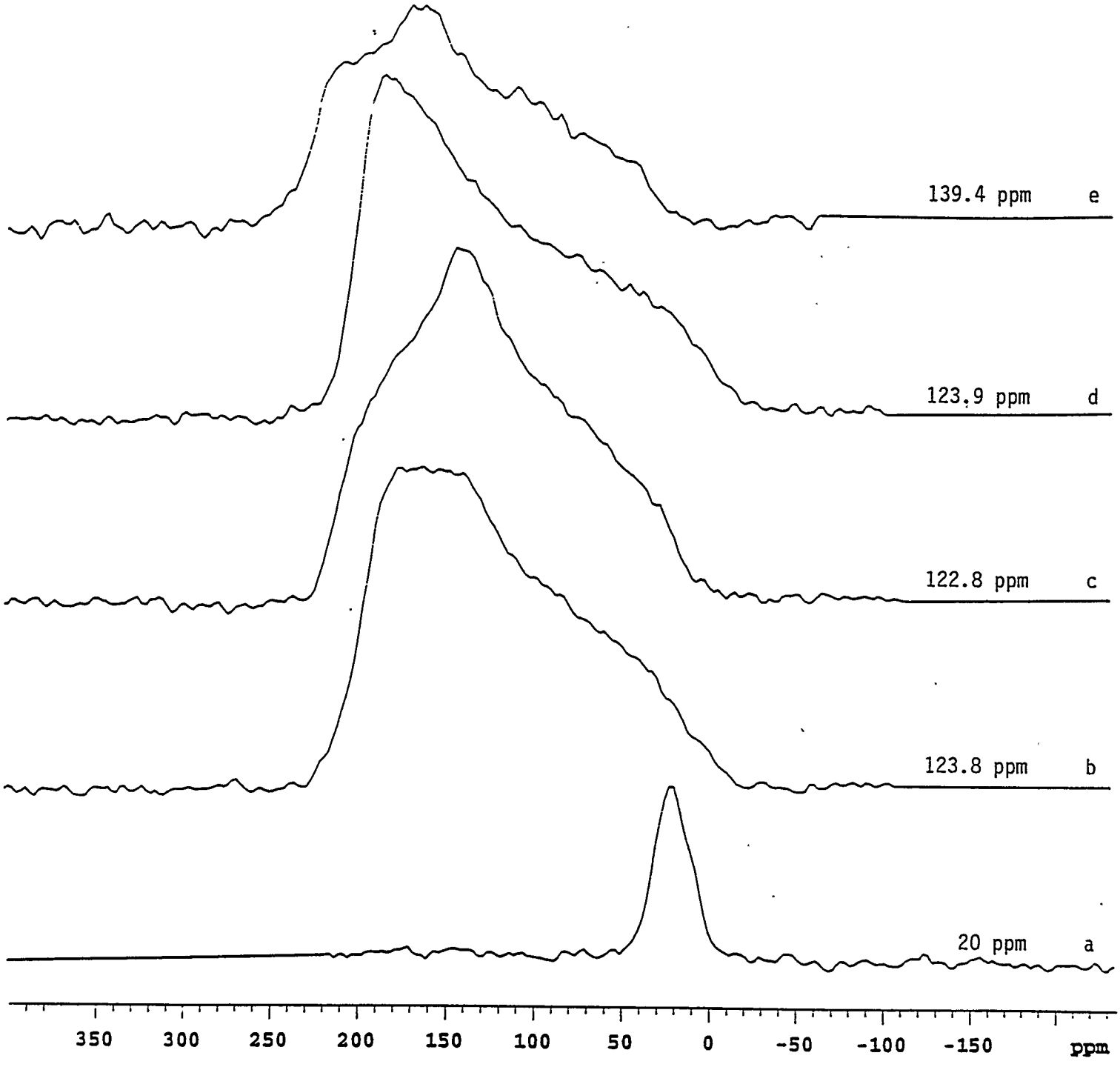

Figure III.2.7. The powder patterns for several selected isotropic chemical shift positions in Pocahontas coal obtained by different MAT techniques.
(a) and (b) were obtained from Figure 6.
(c) was obtained from a short contact time 3-π MAT experiment with a contact time of 50μs.
(d) and (e) were obtained from a dipolar dephasing 3-π MAT experiment with a dipolar dephasing periods of 2*DD=60μs and p_3=1.5ms.